Flexible Batteries

Deutsche Ausgabe: DOI: 10.1002/ange.201504514
Internationale Ausgabe: DOI: 10.1002/anie.201504514

An Aligned and Laminated Nanostructured Carbon Hybrid Cathode for High-Performance Lithium–Sulfur Batteries**

Qian Sun, Xin Fang, Wei Weng, Jue Deng, Peining Chen, Jing Ren, Guozhen Guan, Min Wang,* and Huisheng Peng**

Abstract: *An aligned and laminated sulfur-absorbed mesoporous carbon/carbon nanotube (CNT) hybrid cathode has been developed for lithium–sulfur batteries with high performance. The mesoporous carbon acts as sulfur host and suppresses the diffusion of polysulfide, while the CNT network anchors the sulfur-absorbed mesoporous carbon particles, providing pathways for rapid electron transport, alleviating polysulfide migration and enabling a high flexibility. The resulting lithium–sulfur battery delivers a high capacity of 1226 mAh g^{-1} and achieves a capacity retention of 75 % after 100 cycles at 0.1 C. Moreover, a high capacity of nearly 900 mAh g^{-1} is obtained for 20 mg cm^{-2}, which is the highest sulfur load to the best of our knowledge. More importantly, the aligned and laminated hybrid cathode endows the battery with high flexibility and its electrochemical performances are well maintained under bending and after being folded for 500 times.*

The attractiveness of flexible electronics resides in their sustainability to deformation as well as potential applications such as roll-up displays and portable and wearable electronic devices.[1–4] On this account, affiliated energy storage accessories with good mechanical flexibility and high performance are on an urgent demand. Currently, lithium-ion batteries are widely used in electronic devices and massive efforts have been devoted to achieving flexibility.[5–8] However, the commercialized lithium-ion batteries with energy densities less than 400 Wh kg^{-1} are unlikely to reach a satisfying longevity for power-consuming flexible devices.[9,10] Therefore, it is of great importance to find an alternative beyond the limitations of lithium-ion batteries.

In this case, the lithium–sulfur battery, having intrinsic merits of high energy density (2600 Wh kg^{-1}) and specific capacity (1675 mAh g^{-1}) several times higher than those of the lithium-ion batteries, is a promising candidate. Unfortunately, the lithium–sulfur battery still suffers from several problems that obstruct their commerzialization. For example, the elemental sulfur is insulated and its lithiated intermediates, soluble polysulfides, are prone to leak into the electrolyte. Once the lithium–sulfur compounds diffuse and migrate between the cathode and anode, capacity degradation and battery depletion ensue over the repeated charge–discharge cycles.[11] Fortunately, over the years, the problem of battery degradation has been alleviated and the lifespan has been significantly prolonged. This success has benefited from the introduction of specifically designed sulfur cathodes which are constructed from various materials including inorganics, polymers and carbonaceous materials. Amongst them, carbon nanomaterials are widely appreciated because of their large specific surface area, high electrical conductivity and diverse architectures.[12–16]

Moreover, the application of carbon nanomaterials has underpinned the development of flexible lithium–sulfur batteries.[17] In particular, carbon nanotube (CNT) and graphene films provide a flexible platform for batteries.[2] However, until now, flexibility and electrochemical performance are contradictory, and trade-offs had to be made,[18,19] e.g., relatively fast capacity decay and low sulfur load while achieving high flexibility.

As a tentative step, we create a high-performance and highly flexible lithium–sulfur battery relying on a hybrid

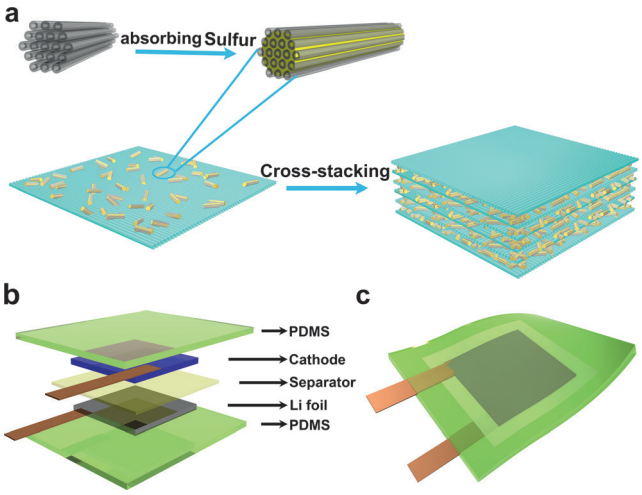

Figure 1. a) Fabrication process of the laminated hybrid sulfur cathode. b, c) Exploded and general views of the flexible lithium–sulfur battery, respectively. Two brown straps made of copper serve as leads for the anode and cathode.

[*] Q. Sun, X. Fang, Dr. W. Weng, J. Deng, P. Chen, J. Ren, G. Guan, Dr. M. Wang, Dr. H. Peng
State Key Laboratory of Molecular Engineering of Polymers, Department of Macromolecular Science, and Laboratory of Advanced Materials, Fudan University, Shanghai 200438 (China)
E-mail: gotovic@163.com
minwang@fudan.edu.cn
penghs@fudan.edu.cn

[**] This work was supported by: MOST (2011CB932503), NSFC (21203033, 21225417), STCSM (12nm0503200), the Fok Ying Tong Education Foundation, the Program for Special Appointments of Professors at Shanghai Institutions of Higher Learning, and the Program for Outstanding Young Scholars from the Organization Department of the CPC Central Committee.

Supporting information for this article is available on the WWW under http://dx.doi.org/10.1002/anie.201504514.

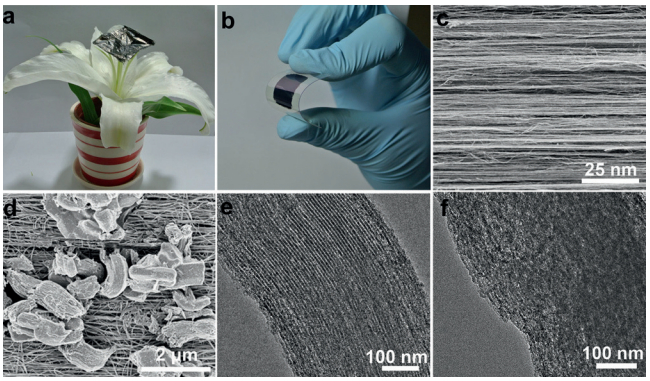

Figure 2. a, b) Photographs of hybrid electrodes being lifted up by a tender flower and being bent into a curved structure, respectively. c, d) Scanning electron microscopy (SEM) images of aligned CNT sheets before and after deposition of CMK-3@S particles, respectively. e, f) Transmission electron microscopy (TEM) images of a bare CMK-3 particle and a CMK-3@S particle with weight ratio of 1:3, respectively.

sulfur cathode with an aligned and laminated nanocarbon structure. Specifically, sulfur is stored in the nano-channels of mesoporous carbon (i.e., CMK-3) particles, resulting in CMK-3@S particles. Aligned CNT sheets serve as conductive and flexible scaffolds, on which CMK-3@S particles are anchored, producing CMK-3@S/CNT sheets. Finally, by cross-stacking the CMK-3@S/CNT sheets layer by layer, a hybrid cathode with a laminated structure is obtained. The CMK-3 particles act as the sulfur host. The aligned CNTs provide effective pathways for electron transport and lithium-ion migration, making the cathode exempt from conductive additives. The laminated CNT scaffolds on one hand endow the cathode with high mechanical strength and flexibility; on the other hand, they perform as physical barriers to suppress the soluble polysulfides spilling from the cathode. As expected, the battery stably runs for hundreds of cycles with a high specific capacity, and it is capable of loading a high sulfur content of 20 mg cm^{-2}. Moreover, it exhibits an endurance to deformation even at a bending angle of 180°.

The preparation of the hybrid cathode is illustrated in Figure 1a. The sulfur was absorbed into the CMK-3 particles by heating at 160 °C. The CMK-3@S particles were then dispersed in ethanol to form a suspension. An aligned CNT sheet of about 100 nm was paved as scaffolds, on which the suspension was deposited. Here the aligned CNT sheets were directly drawn from the spinnable CNT array[20] and a single-layer aligned CNT sheet is lightweight (ca. 8 mg cm^{-3}), ultrathin (ca. 20 nm) and highly conductive (10^2–10^3 S cm^{-1}).[21] The CNT sheets were densified due to the surface tension of solvent. After the solvent was evaporated, the CMK-3@S particles were hedged in the CNT scaffolds, leading to a CMK-3@S/CNT hybrid sheet.[22] Afterwards, the hybrid cathode with a laminated structure was fabricated by cross-stacking the CMK-3@S/CNT sheets. The areal mass density of the sulfur can be simply adjusted by the number of the stacked layers. As for the flexible battery, its assembly is shown in Figure 1b. The free-standing hybrid cathode was transferred to a flexible polydimethylsiloxane (PDMS) substrate. Lithium foil serving as the anode was placed on the other PDMS substrate. The two electrodes separated by a polyolefin membrane were stacked together and the battery was finally sealed also by PDMS, resulting in a flexible lithium–sulfur battery (Figure 1c).

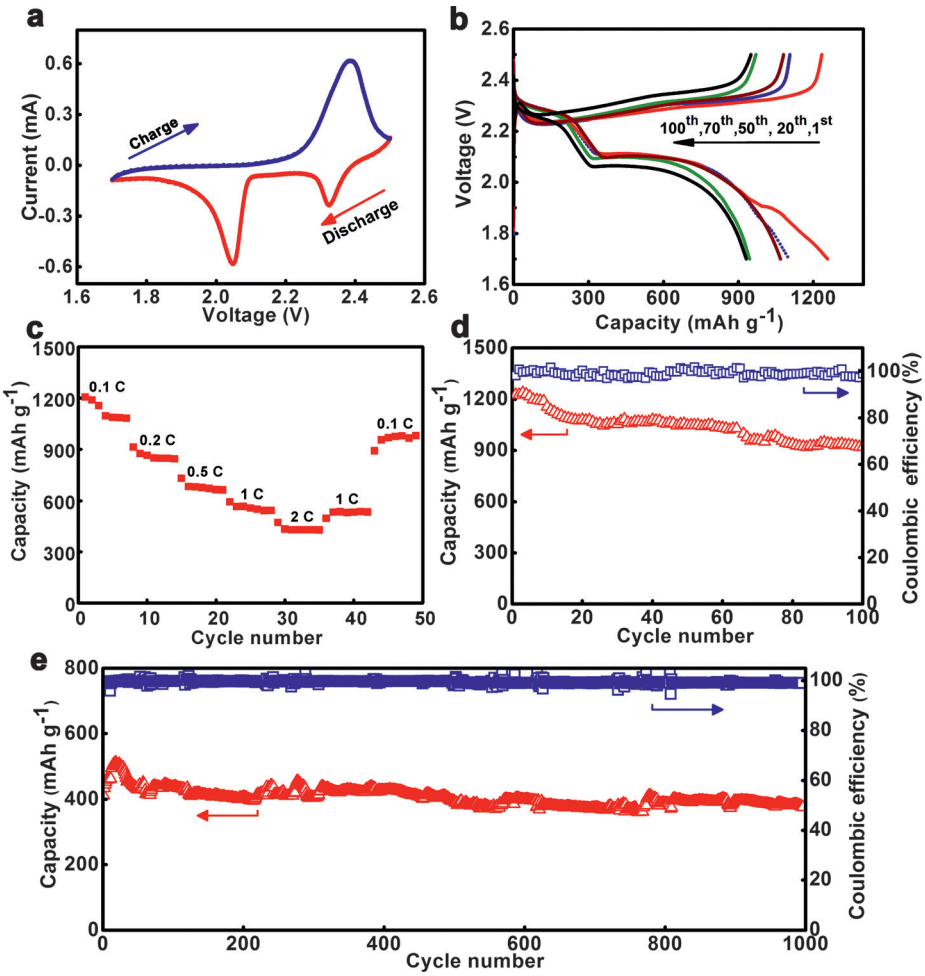

Figure 3. Electrochemical performance of the aligned and laminated nanostructured carbon hybrid cathode with a sulfur load of 1 mg cm^{-2}. a) Cyclic voltammograms at 0.1 mV s^{-1}. b) Voltage profiles at 0.1 C. c) Rate capability. d) Cyclic performance at 0.1 C for 100 cycles. e) Cyclic performance at 2 C for 1000 cycles.

Inheriting the merits of its components-CMK-3 particles and CNT sheets, the hybrid cathode is lightweight, self-standing and flexible in absence of conductive additives and binders (Figure 2a,b). The CNT sheet presents a high alignment (Figure 2c), which was well preserved after the deposition of CMK-3@S particles (Figure 2d). The morphology of a bare CMK-3 particle is shown in Figure 2e, from which the featured channels are distinct. After blended with sulfur, the channels are clearly stuffed with the sulfur (Figure 2f). Moreover, the sulfur content in the channels has an upper limit. Specifically, given the pore volume of CMK-3 particle ($1.6\ cm^3 g^{-1}$) and density of liquid sulfur ($1.82\ g cm^{-3}$), the upper limit of sulfur content in CMK-3@S was deduced as 75 wt% providing that all the pores of CMK-3 particle were filled.[23] In Figure 2f, the weight ratio of CMK-3/S is 1:3. As a comparison, CMK-3@S particles with CMK-3/S weight ratios of 1:2 and 1:4 are shown in Figure S1a and S1b (see Supporting Information), respectively. At a weight ratio of 1:2 the channels were not fully occupied with the sulfur (Figure S1a). Otherwise, at a weight ratio of 1:4, the channels are indiscernible (Figure S1b), suggesting that the sulfur has occupied the vacancies of CMK-3 particles and even spilled out (Figure S1c). X-ray diffraction patterns of CMK-3 particles and CMK-3@S particles with different CMK-3/S weight ratios are shown in Figure S2. Peaks are found to correspond to either CMK-3 or sulfur. No other materials were found. The intensity of peak corresponding to crystalline sulfur is strengthened with the increasing sulfur content, while that of the characteristic peak of CMK-3 is weakened accordingly. The weight ratio of CMK-3/S would affect the electrochemical performance of the hybrid cathode (Figure S3). Since the weight ratio of 1:3 produced the highest performance, this ratio was adopted in the following study.

To evaluate the electrochemical performance of the hybrid cathode, we carried out a series of electrochemical tests. The cyclic voltammogram (CV) in Figure 3a exhibits cathodic peaks at 2.1 and 2.3 V which are in line with the voltage plateaus in Figure 3b. The lower plateau at 2.1 V contributes a major fraction of the capacity and corresponds to the deposition of lower-order lithium sulfur compounds that are insoluble in the electrolyte. The upper plateau at 2.3 V is related to the dissolution of sulfur, i.e., the formation of higher-order polysulfides. After running for 100 cycles, the voltage profile retained its shape with a slightly descending plateau arising from the polarization.[24,25]

The CMK-3@S/CNT hybrid cathode exhibits a decent rate performance (Figure 3c). It has stepwise capacities of 1206, 912, 729, 593 and 473 $mAh g^{-1}$ at 0.1, 0.2, 0.5, 1, and 2 C, respectively. Furthermore, after running at high rates, the battery recovered its capacity of 496 $mAh g^{-1}$ at 1 C and 955 $mAh g^{-1}$ at 0.1 C, manifesting that the hybrid cathode has a good reversibility. As the lithium–sulfur battery suffers from insufficient long-life performance, any improvement should be qualified by the betterment in cyclic performance. Figure 3d shows the long-life performance of the CMK-3@S/CNT hybrid cathode at 0.1 C. The battery delivered a discharge capacity of 1226 $mAh g^{-1}$ at the first cycle, which is 74% of the theoretical value. After draining and recharging for 100 cycles, a capacity of 919 $mAh g^{-1}$ remained, indicating a retention of 75%. Furthermore, the battery had been cycled for 1000 cycles at 2 C, delivering stable capacities around 400 $mAh g^{-1}$ (Figure 3e). It can be concluded that the aligned

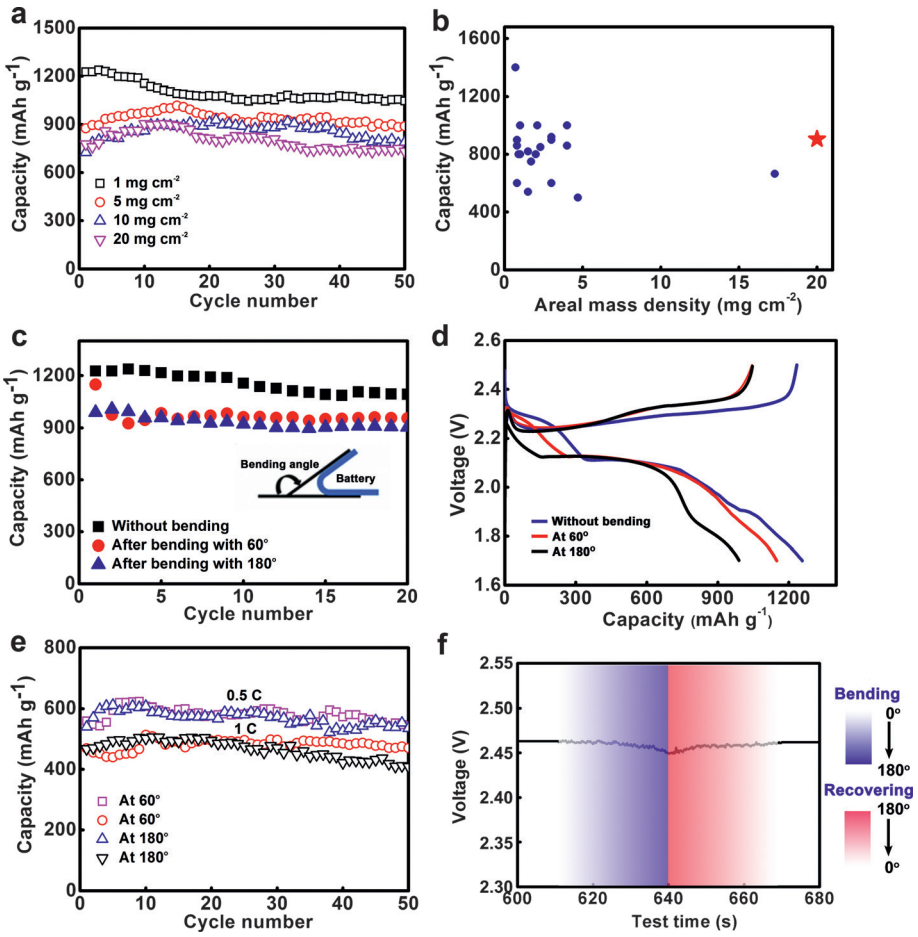

Figure 4. Merits of the lithium–sulfur battery. a) Cyclic performance of the batteries with sulfur loads of 1, 5, 10 and 20 $mg cm^{-2}$ at 0.1 C. b) A comparison on the specific capacity and sulfur load between this battery and the reported lithium–sulfur batteries. c) Cyclic performance of the battery at 0.1 C after bending for 500 times with bending angles of 60° and 180°. d) Voltage profiles at 0.1 C at a bent state with bending angles of 60° and 180°. e) Cyclic performance at 0.5 C and 1 C at a bent state with bending angles of 60° and 180°. f) Real-time monitoring of the voltage of the battery when undergoing bending and recovering.

and laminated CMK-3@S/CNT hybrid cathode has a remarkable performance for energy uptake and delivery, making it eligible for applications. Note that CNT sheets could be further covered on the cathode to enhance the capacity retention (Figure S4).

Sulfur load is a pivotal parameter for a lithium–sulfur battery, which is basically required to be more than 6 mg cm^{-2} to outperform the state-of-the-art lithium-ion batteries. However, areal mass densities of less than 4 mg cm^{-2} were studied in most reports.[26] Here, the areal mass density of sulfur can be flexibly controlled by adjusting the stacking number of CMK-3@S/CNT sheets. The electrochemical performances for the batteries with the sulfur loads of 1, 5, 10 and 20 mg cm^{-2} at 0.1 C are shown in Figure 4a. All of them have a stable cyclic performance. Although the specific capacity was slightly decreased with the increasing areal mass density, a large capacity of nearly 900 mAh g^{-1} was obtained for 20 mg cm^{-2}, which is the highest sulfur load to the best of our knowledge. A comparison on the specific capacity and sulfur load with the previously reported lithium–sulfur batteries[4,12,14,15,18,19,27–41] demonstrates a much higher ability of incorporating more sulfur in this battery (Figure 4b).

Moreover, this battery possesses a high flexibility and can bear a bending angle of as high as 180° (inset of Figure 4c). The electrochemical performance of the battery after bending for 500 times is shown in Figure 4c. The slight decrease in capacity after bending is probably caused by the disconnection of active materials during deformation. But we found that the bending angle has negligible effect on such capacity decay, which suggests a high sustainability to bending deformations. The electrochemical properties were also investigated when the battery was kept at a bent state. The voltage profiles are compared for the batteries without bending and after bending to 60° and 180° (Figure 4d). The voltage plateau at 2.1 V is clearly maintained at bending angles of both 60° and 180°, revealing that the bending operation has little influence on redox reactions. Furthermore, the cyclic performance of the batteries at a bent state was shown to be as stable as the one without bending (Figure 4e). The battery was also monitored in situ when undergoing bending (Figure 4f). The voltage fluctuation was recorded to be less than 0.6%, making the battery suitable for various flexible applications.

For a direct demonstration, a film battery with a high working voltage is shown in Figure 5. It consists of two serially connected lithium–sulfur batteries. The voltage is stable when bending and recovering (Figure 5a–d), and the output of the battery can stably lighten nine light-emitting diodes at one time when bending and recovering (Figure 5e). In a word, the designed lithium–sulfur battery can sustain a rough bending operation, which is mainly ascribed to the novel carbon nanomaterial/sulfur cathode.

Compared with previous reports,[12,18,27,29,38] this work represents a solid progress in cathode design to realize high sulfur load, flexibility and cyclic stability. These advantages are derived from the aligned and laminated structure of the hybrid cathode, proving an effective strategy to solve the longstanding instability problem and create flexible lithium sulfur batteries. For a direct comparison, a cathode without

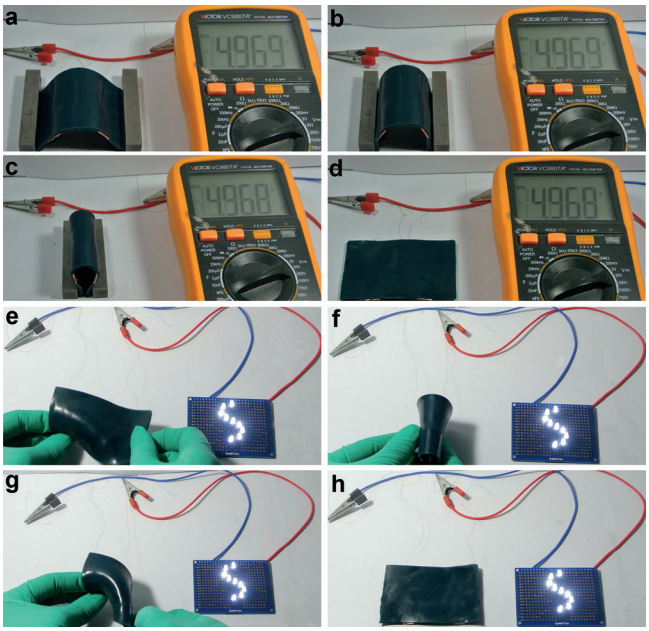

Figure 5. Exhibition of the flexibility of lithium–sulfur battery. a–d) Voltage output when bending and recovering. e–h) Lighting up nine light-emitting diodes when bending and recovering. Here the bottle-green film battery contains two lithium–sulfur batteries connected in series.

laminated structure (Figure S5) exhibited inferior electrochemical performances (Figure 6a and S6a). With the increasing areal sulfur load, the capacity retention decreases, i.e., 76%, 60% and 50% for 1, 5 and 10 mg cm^{-2} after 50 cycles at 0.1 C, respectively. In stark contrast, the cathode with laminated structure shows a capacity retention of 83% at high sulfur load of 20 mg cm^{-2}. The laminated structure also contributes to the deformation stability of the cathode. As shown in Figure 6b and S6b, when the battery was folded, the laminated structure endowed the cathode with a more stable capacity while the cathode without laminated structure suffered severe degradation.

The alignment in cathode plays a pivotal role, too. Traditionally, as the scaffold of active materials, random CNTs have been used for constructing flexible lithium–sulfur batteries.[4,12,15,29,33] To highlight the merit of the aligned structure, as a comparison, we deposited CMK-3@S particles on a random CNT paper to prepare another type of hybrid cathodes (Figure S7). The resulting lithium–sulfur battery showed inferior cyclic stability. Specifically, capacity retention decreased from 58% and 50% to 47% with increasing sulfur loads from 1 and 5 to 10 mg cm^{-2}, respectively (Figure 6c and S6c). The randomly arranged CNTs are also responsible for the much lower deformation stability and rate performances (Figure 6d, S6d and 6e). The aligned CNTs, on the one hand, construct a strong and flexible platform for the battery, and on the other hand they are efficient to transport electrons and lithium ions (Figure 6f).

In summary, we have developed a CMK-3@S/CNT hybrid cathode with laminated structure for a flexible lithium–sulfur battery. Aligned CNT scaffolds play a pivotal role in conducting electrons, retaining capacity, and providing integrity and flexibility. The laminated structure affords the

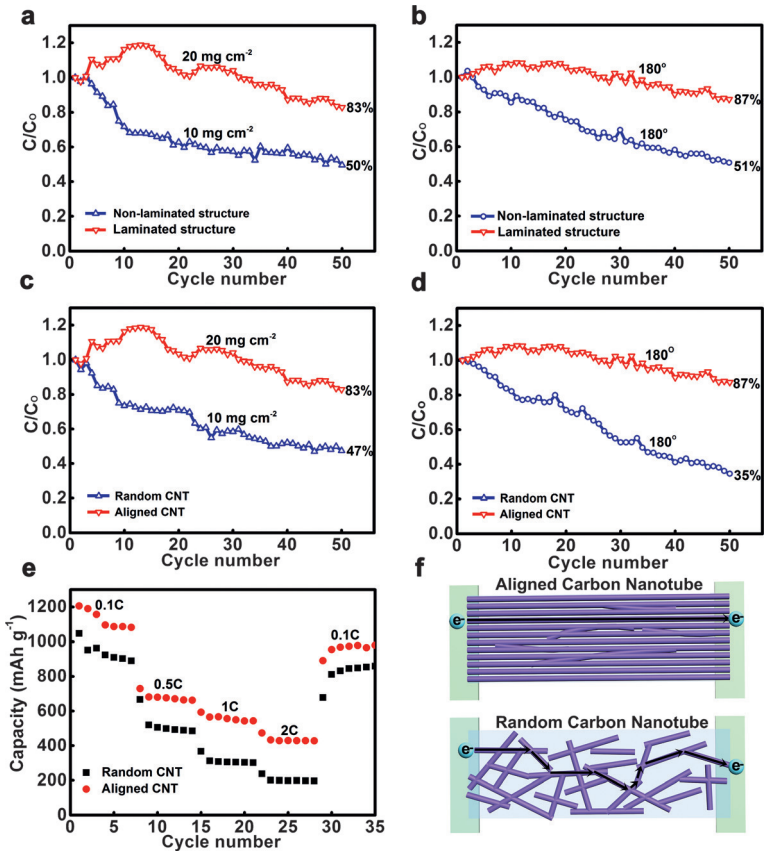

Figure 6. a) Comparison on capacity retention for the batteries without and with the laminated structure at 0.1 C. b) Comparison on capacity retention for the batteries without and with the laminated structure at a bent state at 1 C. c) Comparison on capacity retention for the batteries using random and aligned CNTs at 0.1 C. d) Comparison on capacity retention for the batteries using random and aligned CNTs at a bent state at 1 C. e) Comparison on the rate performance of the batteries using random and aligned CNTs. f) Schematic illustration on the comparison of electron transport through random and aligned CNT materials. The sulfur loads for hybrid cathodes in (b), (d) and (e) are the same of 1 mg cm^{-2}.

cathode a high sulfur load up to 20 mg cm^{-2}. The designed lithium–sulfur battery shows remarkable electrochemical performances including high specific capacity and decent capacity retention, e.g., it can stably run for 1000 cycles at high rates. Moreover, the hybrid cathode affords the battery high flexibility that enables itself to sustain deformations. This work presents an effective strategy to upgrade the powering systems of flexible devices and provides promising results for the practical application of lithium–sulfur batteries.

Keywords: carbon nanotubes · flexible devices · lithium–sulfur battery · mesoporous carbon

How to cite: *Angew. Chem. Int. Ed.* **2015**, *54*, 10539–10544
Angew. Chem. **2015**, *127*, 10685–10690

[1] W. Zeng, L. Shu, Q. Li, S. Chen, F. Wang, X.-M. Tao, *Adv. Mater.* **2014**, *26*, 5310–5336.
[2] X. Wang, X. Lu, B. Liu, D. Chen, Y. Tong, G. Shen, *Adv. Mater.* **2014**, *26*, 4763–4782.
[3] K. Xie, B. Wei, *Adv. Mater.* **2014**, *26*, 3592–3617.
[4] J. Huang, H. Peng, X. Liu, J. Nie, X. Cheng, Q. Zhang, F. Wei, *J. Mater. Chem. A* **2014**, *2*, 10869–10875.
[5] W. Weng, H. Lin, X. Chen, J. Ren, Z. Zhang, L. Qiu, G. Guan, H. Peng, *J. Mater. Chem. A* **2014**, *2*, 9306–9312.
[6] K. Fu, O. Yildiz, H. Bhanushali, Y. Wang, K. Stano, L. Xue, X. Zhang, P. D. Bradford, *Adv. Mater.* **2013**, *25*, 5109–5114.
[7] N. Li, Z. Chen, W. Ren, F. Li, H.-M. Cheng, *Proc. Natl. Acad. Sci. USA* **2012**, *109*, 17360–17365.
[8] S. Xu, Y. Zhang, J. Cho, J. Lee, X. Huang, L. Jia, J. A. Fan, Y. Su, J. Su, H. Zhang, H. Cheng, B. Lu, C. Yu, C. Chuang, T.-i. Kim, T. Song, K. Shigeta, S. Kang, C. Dagdeviren, I. Petrov, P. V. Braun, Y. Huang, U. Paik, J. A. Rogers, *Nat. Commun.* **2013**, *4*, 1543.
[9] M. M. Thackeray, C. Wolverton, E. D. Isaacs, *Energy Environ. Sci.* **2012**, *5*, 7854–7863.
[10] C.-X. Zu, H. Li, *Energy Environ. Sci.* **2011**, *4*, 2614–2624.
[11] A. Manthiram, Y. Fu, S.-H. Chung, C. Zu, Y.-S. Su, *Chem. Rev.* **2014**, *114*, 11751–11787.
[12] W. Bao, Z. Zhang, C. Zhou, Y. Lai, J. Li, *J. Power Sources* **2014**, *248*, 570–576.
[13] C. Zhang, H. B. Wu, C. Yuan, Z. Guo, X. W. Lou, *Angew. Chem. Int. Ed.* **2012**, *51*, 9592–9595; *Angew. Chem.* **2012**, *124*, 9730–9733.
[14] H. Wang, Y. Yang, Y. Liang, J. T. Robinson, Y. Li, A. Jackson, Y. Cui, H. Dai, *Nano Lett.* **2011**, *11*, 2644–2647.
[15] Z. Yuan, H.-J. Peng, J.-Q. Huang, X.-Y. Liu, D.-W. Wang, X.-B. Cheng, Q. Zhang, *Adv. Funct. Mater.* **2014**, *24*, 6105–6112.
[16] L. Sun, W. B. Kong, Y. Jiang, H. C. Wu, K. L. Jiang, J. P. Wang, S. S. Fan, *J. Mater. Chem. A* **2015**, *3*, 5305–5312.
[17] X. Fang, H. Peng, *Small* **2014**, *10*, 1488–1511.
[18] L. C. Zeng, F. S. Pan, W. H. Li, Y. Jiang, X. W. Zhong, Y. Yu, *Nanoscale* **2014**, *6*, 9579–9587.
[19] J. Song, Z. Yu, T. Xu, S. Chen, H. Sohn, M. Regula, D. Wang, *J. Mater. Chem. A* **2014**, *2*, 8623–8627.
[20] S. Huang, Z. Yang, L. Zhang, R. He, T. Chen, Z. Cai, Y. Luo, H. Lin, H. Cao, X. Zhu, H. Peng, *J. Mater. Chem. A* **2012**, *22*, 16833–16838.
[21] Z. Yang, T. Chen, R. He, G. Guan, H. Li, L. Qiu, H. Peng, *Adv. Mater.* **2011**, *23*, 5436–5439.
[22] X. Sun, T. Chen, Z. Yang, H. Peng, *Acc. Chem. Res.* **2012**, *46*, 539–549.
[23] L. Suo, Y. Hu, H. Li, M. Armand, L. Chen, *Nat. Commun.* **2013**, *4*, 1481–1489.
[24] Y. V. Mikhaylik, J. R. Akridge, *J. Electrochem. Soc.* **2004**, *151*, A1969–A1976.
[25] S. S. Zhang, *J. Power Sources* **2013**, *231*, 153–162.
[26] M. Hagen, D. Hanselmann, K. Ahlbrecht, R. Maça, D. Gerber, J. Tübke, *Adv. Energy Mater.* **2015**, DOI: 10.1039/C4A00245h.
[27] J. Schuster, G. He, B. Mandlmeier, T. Yim, K. T. Lee, T. Bein, L. F. Nazar, *Angew. Chem. Int. Ed.* **2012**, *51*, 3591–3595; *Angew. Chem.* **2012**, *124*, 3651–3655.
[28] G. Zhou, L. Li, D. W. Wang, X. Y. Shan, S. Pei, F. Li, H. M. Cheng, *Adv. Mater.* **2015**, *27*, 641–647.
[29] G. Zhou, D. Wang, F. Li, P. Hou, L. Yin, C. Liu, G. Lu, I. R. Gentle, H. Cheng, *Energy Environ. Sci.* **2012**, *5*, 8901–8906.
[30] C. Wang, K. Su, W. Wan, H. Guo, H. Zhou, J. Chen, X. Zhang, Y. Huang, *J. Mater. Chem. A* **2014**, *2*, 5018–5023.

[31] Q. Zhao, X. Hu, K. Zhang, N. Zhang, Y. Hu, J. Chen, *Nano Lett.* **2015**, *15*, 721 – 726.
[32] C. Wang, X. Wang, Y. Yang, A. Kushima, J. Chen, Y. Huang, J. Li, *Nano Lett.* **2015**, *15*, 1796 – 1802.
[33] K. Jin, X. Zhou, L. Zhang, X. Xin, G. Wang, Z. Liu, *J. Phys. Chem. C* **2013**, *117*, 21112 – 21119.
[34] X. Zhou, J. Xie, J. Yang, Y. Zou, J. Tang, S. Wang, L. Ma, Q. Liao, *J. Power Sources* **2013**, *243*, 993 – 1000.
[35] Y. Chen, S. Lu, X. Wu, J. Liu, *J. Phys. Chem. C* **2015**, *119*, 10288 – 10294.
[36] H. Nagata, Y. Chikusa, *J. Power Sources* **2014**, *264*, 206 – 210.
[37] X. Y. Zhao, J. P. Tu, Y. Lu, J. B. Cai, Y. J. Zhang, X. L. Wang, C. D. Gu, *Electrochim. Acta* **2013**, *113*, 256 – 262.
[38] X. Wang, Z. Wang, L. Chen, *J. Power Sources* **2013**, *242*, 65 – 69.
[39] F. Wu, L. Shi, D. Mu, H. Xu, B. Wu, *Carbon* **2015**, *86*, 146 – 155.
[40] G. Yuan, G. Wang, H. Wang, J. Bai, *J. Solid State Electrochem.* **2015**, *19*, 1143 – 1149.
[41] Q. Long, M. Arumugam, *Adv. Mater.* **2015**, *27*, 1694 – 1700.

Received: May 19, 2015
Published online: July 14, 2015